Physics-informed neural networks for one-dimensional heat transfer in climate models

Marat Nurtas[1,2,†], Aizhan Ydyrys[1,*,†] and Zhanibek Ydyrys[1,†]

[1] International Information Technology University, 34/1 Manas St., Almaty, Kazakhstan
[2] Institute of Ionosphere, Gardening community IONOSPHERE 117, Almaty, 050020, Kazakhstan

Abstract
This paper presents an application of physics-informed neural networks (PINNs) to the classical one-dimensional heat equation, a fundamental model for describing thermal diffusion processes relevant to climate systems. Using synthetically generated data, we demonstrate the effectiveness of PINN in accurately approximating analytical solutions and incorporating observational information, thus laying the foundation for their application to more complex climate modeling scenarios. Our approach specifically investigates the impact of a balanced multi-component loss function and a hybrid data-collocation strategy on the model's accuracy and physical consistency in the presence of noise.

Keywords
physics-informed neural networks, one-dimensional heat equation, loss balancing, synthetic data, climate modeling

1. Introduction

The precise representation of the climate system and the forecast of its future states are two central tasks in climate science, both of which rely on accurately capturing the complex interactions among mass, momentum, and energy, typically described by nonlinear partial differential equations (PDE) and solved numerically in climate models [1]. Common numerical methods -by which these PDEs are discretized over space and time - include finite difference methods, finite volume methods, where spatial derivatives are approximated using values at grid points or control volumes, and spectral methods [2, 3, 4]. These numerical methods form the basis for dynamic weather and climate modeling, allowing a physically consistent modeling of atmospheric processes in complex terrain and over time, as well as sensitivity analysis, integrated forecasting, and quantification of uncertainty, which are necessary for reliable forecasting in chaotic systems. However, numerical modeling has a significant computational cost, is highly sensitive to initial conditions, and often depends on incomplete representations of physical processes, particularly when fine resolution is needed to capture local climate dynamics [5, 6].

To address these limitations, machine learning (ML) has emerged as a powerful tool in climate science. ML offers a flexible framework for analyzing large climate datasets, learning predictive representations directly from data, and complementing or accelerating traditional numerical models in both forecasting and climate modeling tasks [7, 8]. ML approaches can supplement these traditional methods by offering data-driven alternatives or hybrid models that aim to balance computational efficiency with predictive accuracy. In particular, physics-informed neural networks (PINNs) have garnered considerable attention for their novel integration of physical laws directly into the architecture of neural networks [9]. Unlike conventional data-driven models that approximate mass and momentum conservation using predefined basis functions, PINNs incorporate physical constraints into the training process, including the Navier–Stokes equations and

[1] *AI 2025: Workshop on Artificial Intelligence, November 19-20, 2025, Almaty, Kazakhstan*
* Corresponding author.
† These authors contributed equally.
m.nurtas@iitu.edu.kz (M. Nurtas); a.ydyrys@iitu.edu.kz (A. Ydyrys); zh.ydyrys@iitu.edu.kz (Zh. Ydyrys)
0000-0003-4351-0185 (M. Nurtas); 0000-0002-4284-9446 (A. Ydyrys); 0009-0001-1124-4364 (Zh. Ydyrys)
© 2025 Copyright for this paper by its authors. Use permitted under Creative Commons License Attribution 4.0 International (CC BY 4.0).

CEUR Workshop Proceedings ceur-ws.org ISSN 1613-0073
published 2026-07-16

CEUR-WS.org/Vol-4224/ShortPaper2.pdf

thermodynamic principles. This approach reduces the amount of training data required while improving the physical consistency and generalizability of the predictions [10, 11].

PINNs present a compelling solution to the inherent limitations of traditional PDE solvers, particularly in cases where observational data is sparse, incomplete, or prohibitively expensive to collect, a common scenario in climate modeling [10]. Furthermore, PINNs are naturally suited for solving both forward (predictive) and inverse (parameter estimation) problems, making them powerful tools for simulating climate dynamics and inferring unknown physical parameters from available data [12].

This paper provides a focused study of PINNs applied to the classical one-dimensional heat equation, a fundamental model for describing thermal diffusion processes relevant to climate systems. While the application of PINNs to simple PDEs is established, our work contributes by systematically evaluating a strategy for integrating sparse and noisy synthetic observations within a structured loss function. The novelty of our approach lies in:

1. The implementation and analysis of a composite loss function that carefully balances the PDE residual, initial/boundary conditions, and observational data loss, which is crucial for stable convergence when data is imperfect;
2. A hybrid collocation strategy that uses uniformly sampled points for physics enforcement and a separate, sparser set of noisy spatial-temporal points for data assimilation, mimicking real-world data scarcity;
3. A demonstration of how this framework maintains physical consistency while fitting noisy data, providing a foundation for future applications to real climate data inversion and parameter estimation problems.

Using synthetically generated data, we demonstrate the effectiveness of PINNs in accurately approximating analytical solutions and incorporating observational information, thereby laying the foundation for their application to more complex climate modeling scenarios.

2. Problem formulation: 1D heat equation

We consider the transient one-dimensional heat equation in the domain $x \in [0,1], t \in [0,1]$:

$$\frac{\partial T(x,t)}{\partial t} = k \frac{\partial^2 T(x,t)}{\partial x^2} + Q(x,t), \tag{1}$$

where $T(x,t)$ denotes the temperature (in °C), $k>0$ is the constant thermal diffusivity, and $Q(x,t)$ represents an external heat source. In this study, we set $Q(x,t) \equiv 0$ so that an analytical reference solution is available; specifically, when the initial condition is chosen as $T_0(x) = \sin(\pi x)$, the exact solution is

$$T_{exact}(x,t) = e^{-k\pi^2 t} \sin(\pi x).$$

Homogeneous Dirichlet boundary conditions are imposed at $x=0$ and $x=1$,

$$T(0,t)=0, T(1,t)=0, t \in [0,1],$$

and the initial temperature profile is prescribed by

$$T(x,0) = \sin(\pi x), x \in [0,1].$$

Under these conditions, the one-dimensional heat equation admits a closed-form solution that serves as the basis for generating synthetic observations. Collocation points are uniformly sampled on $[0,1]\times[0,1]$ to enforce residual PDE through automatic differentiation in the PINN framework. The residual at each collocation point (x,t) is defined by

$$R(x,t)=\frac{\partial \hat{T}}{\partial t}(x,t)-k\frac{\partial^2 \hat{T}}{\partial x^2}(x,t), \tag{2}$$

and the corresponding PDE-loss term is the mean squared residual over all collocation points. The initial and boundary conditions are enforced by minimizing the mean squared error between $\hat{T}(x,0)$ and $\sin(\pi x)$ for $x\in[0,1]$, as well as between $\hat{T}(0,t),\hat{T}(1,t)$ and zero for $t\in[0,1]$.

3. PINN model architecture

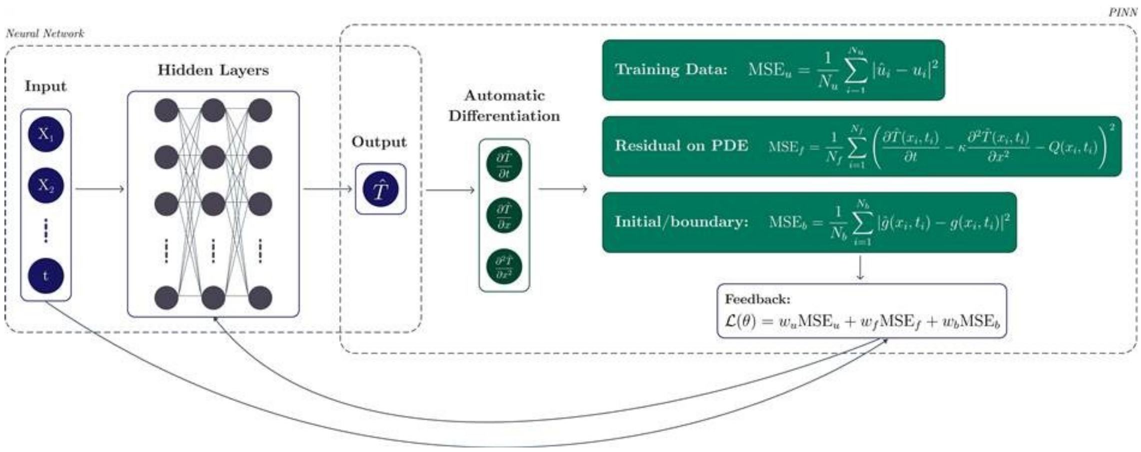

Figure 1: Physics-Informed Neural Network's architecture for the 1D heat equation.

We define a neural network $\hat{T}(x,t)$ that approximates the solution. The loss function includes the following components:

- **PDE Residual:** Enforces the heat equation. The core idea behind PINNs is to embed physical laws directly into the training process. For the 1D heat equation, this is done by minimizing the residual of the governing PDE at a set of collocation points (x_i,t_i) sampled from the spatial–temporal domain. Specifically, we use the definition in Equation (2). During training, the network adjusts its parameters to minimize the mean squared error of $R(x,t)$ at all the location points, ensuring that the learned solution adheres to the physics of the heat equation [12].
- **Initial Condition Loss:** Fits $T(x,0)$. To correctly model the heat equation, it is necessary to enforce the initial temperature distribution at time $t=0$. The initial condition is specified as

$$T(x,0)=T_0(x), \tag{3}$$

where $T_0(x)$ is a known temperature profile in the spatial domain. In the PINN framework, we enforce this by minimizing the mean squared error (MSE) between the predicted temperature $\hat{T}(x,0)$ by the neural network and the true initial condition $T_0(x)$. The loss of the initial condition is defined as

$$L_{IC}=\frac{1}{N_{IC}}\sum_{i=1}^{N_{IC}}\left(\hat{T}(x_i,0)-T_0(x_i)\right)^2,$$

where $\{x_i\}_{i=1}^{N_{IC}}$ are the points sampled in the spatial domain at the time of initial sampling. In practice, this is implemented by:

- Setting the temporal input $t=0$.

- Passing $(x, 0)$ into the neural network to predict $\hat{T}(x, 0)$.
- Calculating the MSE between $\hat{T}(x, 0)$ and the true initial condition values $T_0(x)$.

This approach ensures the consistency of the network with the known physical state of the system at the start of the simulation [9].

- **Boundary Condition Loss:** Fits $T(0, t)$ and $T(1, t)$. Boundary conditions play a vital role in ensuring the physical precision of PINNs. For the one-dimensional heat equation, Dirichlet boundary conditions are imposed at the locations $x=0$ and $x=1$. The loss function for the boundary conditions can be expressed as the mean squared error between the predicted temperatures and the known boundary values.

$$L_{BC}=\frac{1}{N_b}\left(\sum_{i=1}^{N_b}\hat{T}(0,t_i)^2+\sum_{i=1}^{N_b}\hat{T}(1,t_i)^2\right), \tag{4}$$

where N_b represents the number of boundary points sampled at different times t_i. Karniadakis et al. (2021) emphasize that strict enforcement of boundary conditions is crucial to ensure the stability and physical consistency of PINNs [10].

- **Observation Loss:** Fits real NOAA temperature data. To ensure that PINNs generate physically plausible solutions that also align with empirical evidence, the integration of observational data is paramount. This is achieved through the observation loss term, which acts as a direct constraint, guiding the network to learn solutions that not only satisfy the governing physical laws but also accurately reproduce available measurements. The observation loss is defined as:

$$L_{obs}=\frac{1}{N_{obs}}\sum_{i=1}^{N_{obs}}\left(\hat{T}(x_i,t_i)-T_{obs,i}\right)^2. \tag{5}$$

Integrating observational data into the PINN framework not only enhances the accuracy of the model but also provides a mechanism for correcting potential biases or inaccuracies inherent in the physics-based residuals. This approach has been demonstrated in various studies, such as the work by Liu et al. [13], where a PINN-based method was employed for temperature field inversion in heat-source systems, effectively integrating observational data to improve prediction precision.

4. From formulation to implementation: Data integration

Having defined the model architecture and loss components, the next step involves generating and integrating the data needed for training. Synthetic observations are generated by evaluating the exact solution $T_{exact}(x_i, t_j)$ on a uniform grid of points $\{(x_i, t_j)\} \subset [0,1]\times[0,1]\}$. To emulate realistic measurement uncertainty, independent Gaussian noise $\epsilon_{ij} \sim N(0, \sigma^2)$ is added to each value:

$$T_{obs}(x_i,t_j)=T_{exact}(x_i,t_j)+\epsilon_{ij}.$$

A subset of these noisy evaluations is then chosen as the observation set for PINN training; the remaining points (without noise) serve as a validation set to quantify the predictive error against the exact solution. Because all spatial and temporal coordinates lie in $[0,1]$, no further normalization is required for the input of the neural network, and the observed temperatures T_{obs} are used directly in degrees Celsius. To simulate realistic conditions, synthetic observations were generated in tabular form, including geographic coordinates, date, and corresponding surface temperature. A subset of the dataset is shown in Table 1. All data points are fixed in space and span daily measurements, representing a typical midlatitude winter pattern.

During training, the PINN minimizes a composite loss consisting of four components: (i) the residual loss of PDE over the collocation points, (ii) the loss of initial condition enforcing $T(x,0)=\sin(\pi x)$, (iii) the loss of boundary condition enforcing $T(0,t)=0$ and $T(1,t)=0$, and (iv) the term of observation loss in Equation (5), where $\{(x_k,t_k,T_{obs},k)\}$ are noisy temperature samples selected from the synthetic grid. By combining these loss terms, the PINN is guided to produce a solution that respects the heat- equation physics, honors the prescribed initial and boundary conditions, and aligns with the noisy observations. After training converges, the performance is assessed in the validation set by computing the relative L^2 error between $\hat{T}(x_l,t_l)$ and $T_{exact}(x_l,t_l)$, confirming that the PINN has learned the true dynamics of the heat equation under measurement noise.

Table 1

Sample of synthetic observational dataset used in training

Latitude	Longitude	Date	Temperature (°C)
43.0	76.9	2023-01-01	−5.2
43.0	76.9	2023-01-02	−4.8
43.0	76.9	2023-01-03	−3.5
43.0	76.9	2023-01-04	−2.1
43.0	76.9	2023-01-05	0.4
43.0	76.9	2023-01-06	1.2
43.0	76.9	2023-01-07	0.8
43.0	76.9	2023-01-08	−0.5
43.0	76.9	2023-01-09	−1.3
43.0	76.9	2023-01-10	−2.7

Temperature values represent daily surface temperature in °C at a fixed location.

5. Results and performance analysis

Using the methodology described above, the PINN was trained to solve the one-dimensional heat equation under prescribed initial and boundary conditions, with additional synthetic temperature observations. The training process used a stochastic optimizer to minimize the loss of the composite until convergence. In the experiment, collocation points were sampled from the interior of the spatial- temporal domain to enforce the residual of the PDE, while the boundary and initial condition points ensured adherence to the physical constraints. A subset of the analytical solution was used to emulate the observational data.

The PINN rapidly learned the dynamics of the system, accurately reproducing the analytical solution across the domain. The predicted temperature field exhibited smooth spatial and temporal behavior consistent with heat diffusion, and the relative error L^2 remained on the order of 10^{-3}. The boundary and initial conditions were satisfied to within the precision of the machine, and the inclusion of noisy observations improved the generalization of the model without compromising the physical consistency.

The evolution of the predicted temperature field over space and time is visualized in the contour plot in Figure 2, which clearly shows the decaying nature of the initial sinusoidal temperature profile, as expected from the heat equation. In addition, the predictive accuracy of the network over time is confirmed by the time series trace at $x=0.5$ in Figure 3, where the PINN maintains fidelity even beyond the training interval, demonstrating a strong extrapolation capability under physical constraints.

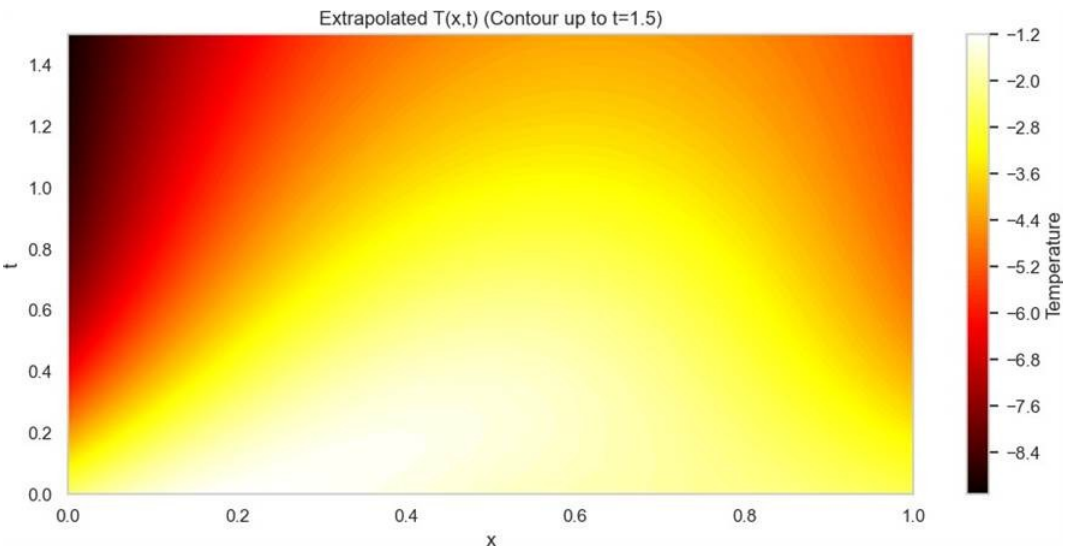

Figure 2: Predicted temperature field $\hat{T}(x,t)$ up to $t=1.5$. The model captures the characteristic behavior of heat diffusion, with temporal decay of the sinusoidal initial condition.

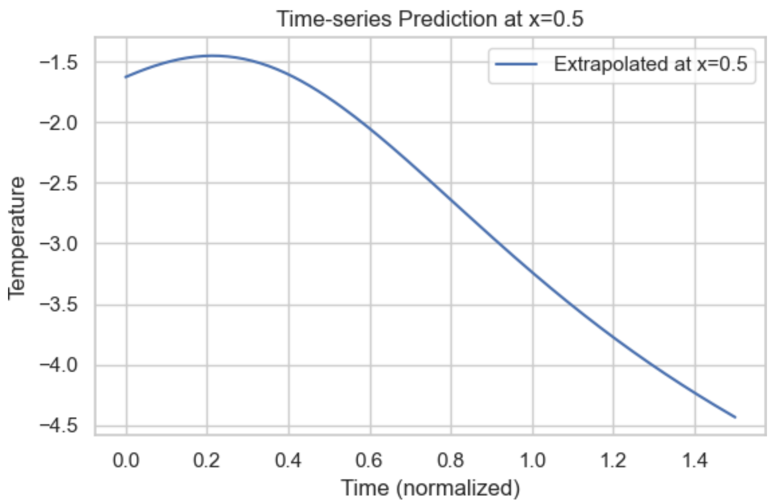

Figure 3: Time-series prediction at $x=0.5$, showing accurate temporal decay of the temperature profile, consistent with the heat equation solution.

6. Discussion

The application of a physics-informed neural network (PINN) to the 1D heat equation demonstrates both its promise and current limitations for climate modeling. Our results show that PINNs can learn a physically consistent solution that respects the governing PDE and boundary conditions, even while incorporating noisy observational data. The model achieved high accuracy (relative error ~ 10^{-3}), highlighting its potential as a high-fidelity surrogate in scenarios where analytical solutions are not available. The successful implementation of our balanced loss function and hybrid collocation strategy was key to this robust performance.

A key strength of PINNs lies in their ability to integrate sparse data without sacrificing physical consistency. This makes them attractive for climate applications, where high-resolution observational datasets are often limited. Our experiment with synthetic observations confirms that a properly constructed PINN can generalize well and reproduce the underlying dynamics from limited, noisy data, in agreement with the findings of other studies [13].

However, scaling PINNs to more complex systems (e.g. 3D atmosphere or ocean models) presents challenges. Training PINNs can be computationally intensive and sensitive to hyperparameters, particularly in high-dimensional or stiff problems. The loss balancing act we performed for this 1D case becomes significantly more complex in multi-physics systems.

Overall, while PINNs are not yet a drop-in replacement for traditional solvers, this study supports their role as a promising complement, especially as climate modeling increasingly turns to hybrid, data-augmented strategies. The framework tested here provides a validated starting point for such hybrid approaches.

7. Conclusion

This study demonstrated the application of physics-informed neural networks (PINNs) to a fundamental partial differential equation relevant to climate modeling, the one-dimensional heat equation. By embedding physical constraints directly into the loss function of a neural network, we trained a PINN that accurately learned the evolution of temperature over space and time, while also integrating synthetic observational data. The model achieved high fidelity to the analytical solution, even under noisy measurements, with relative L^2 errors on the order of 10^{-3}. These results underscore the effectiveness of PINNs in producing physically consistent, data-informed solutions in scenarios where traditional data-driven methods may struggle due to limited or imperfect observations.

The use of PINNs in this setting also highlighted their flexibility and potential advantages: mesh-free formulation, natural handling of initial and boundary conditions, and the ability to incorporate observational data without violating governing physical laws. However, challenges remain in scaling these methods to higher-dimensional and more nonlinear systems typical in climate modeling, where training complexity, computational cost, and loss balancing can become critical issues.

Looking ahead, PINNs show promise for use as surrogate models for subcomponents of climate models, as tools for parameter estimation, or in real-time data assimilation pipelines. To realize this potential and confirm the practical applicability of our approach, future work will focus on testing this PINN framework with real climate data. This will involve applying the model to historical temperature records from sources like NOAA or ERA5 to reconstruct past climate fields or infer unknown parameters. Evaluating the performance of PINNs under these realistic modeling uncertainties and data structures is the essential next step in transitioning this promising methodology from a synthetic testbed to a practical tool for climate science. With continued methodological improvements and validation efforts, physics-informed neural networks may play a key role in advancing the next generation of hybrid climate models that take advantage of both physical theory and data-driven insights.

Declaration on Generative AI

The authors have not employed any Generative AI tools.

References

[1] Geneva N, Zabaras N. Modeling the dynamics of PDE systems with physics-constrained deep auto-regressive networks. *Journal of Computational Physics*, 403, 109056, 2020.

[2] Balcha SK, Hulluka TA, Awass AA, Bantider A, Ayele GT, Walsh CL. Numerical groundwater flow modeling under future climate change in the Central Rift Valley Lakes Basin; Ethiopia. *Journal of Hydrology: Regional Studies*, 52, 101733, 2024. Available at: https://www.sciencedirect.com/science/article/pii/S2214581824000818.

[3] Sweilam NH, Al-Mekhlafi SM, Hassan SM, Alsunaideh NR, Radwan AE. Crossover dynamics of climate change models: Numerical simulations. *Alexandria Engineering Journal*, 75, 447–458, 2023. Available at: https://doi.org/10.1016/j.aej.2022.10.008.

[4] Ovadia O, Oommen V, Kahana A, Peyvan A, Turkel E, Karniadakis GE. Real-time inference and extrapolation with Time-Conditioned UNet: Applications in hypersonic flows, incompressible

flows, and global temperature forecasting. *Computer Methods in Applied Mechanics and Engineering*, 441, 117982, 2025. Available at: https://doi.org/10.1016/j.cma.2024.117982.

[5] Aggarwal R, Kumar R. A comprehensive review of numerical weather prediction models. *Interna- tional Journal of Computer Applications*, 74(18), 44–48, 2013. Available at: https://doi.org/10.5120/ 12989-0246.

[6] Rolnick D, Donti PL, Kaack LH, Kochanski K, Lacoste A, Sankaran K, Ross AS, Milojevic-Dupont N, Jaques N, Waldman-Brown A, et al. Tackling climate change with machine learning. *ACM Computing Surveys*, 55(3), 1–96, 2022. Available at: https://doi.org/10.1145/3485128.

[7] Reichstein M, Camps-Valls G, Stevens B, Jung M, Denzler J, Carvalhais N, Prabhat. Deep learning and process understanding for data-driven Earth system science. *Nature*, 566, 195–204, 2019. Available at: https://www.nature.com/articles/s41586-019-0912-1.

[8] de Burgh-Day CO, Leeuwenburg T. Machine learning for numerical weather and climate modelling: a review. *Geoscientific Model Development*, 16(22), 6433–6477, 2023. Available at: https://doi.org/10. 5194/gmd-16-6433-2023.

[9] Raissi M, Perdikaris P, Karniadakis GE. Physics-informed neural networks: A deep learning framework for solving forward and inverse problems involving nonlinear partial differential equations. *Journal of Computational Physics*, 378, 686–707, 2019.

[10] Karniadakis GE, Kevrekidis IG, Lu L, Perdikaris P, Wang S, Yang L. Physics-informed machine learning. *Nature Reviews Physics*, 3(6), 422–440, 2021.

[11] Fefferman C. Existence and smoothness of the Navier–Stokes equation. Clay Mathematics Institute, 2006. Available at: https://www.claymath.org/sites/default/files/navierstokes.pdf.

[12] Cuomo S, Di Cola VS, Giampaolo F, Rozza G, Raissi M, Piccialli F. Scientific machine learning through physics–informed neural networks: Where we are and what's next. *Journal of Scientific Computing*, 92(3), 88, 2022.

[13] Liu X, Peng W, Gong Z, Zhou W, Yao W. Temperature field inversion of heat-source systems via physics-informed neural networks. *Engineering Applications of Artificial Intelligence*, 113, 104902, 2022.

[14] Flato G, et al. Evaluation of Climate Models. *Climate Change 2013: The Physical Science Basis*, IPCC AR5 Working Group I, Chapter 9, 2013. Available at: https://www.ipcc.ch/site/assets/uploads/2018/ 02/WG1AR5_Chapter09_FINAL.pdf.

[15] Knutti R, Sedláček J. Robustness and uncertainties in the new CMIP5 climate model projections. *Na- ture Climate Change*, 3, 369–373, 2013. Available at: https://www.nature.com/articles/nclimate1716.

[16] Mashakova D., Nurtas M., Ydyrys A., Ipalakova M. Improving Weather-sensing Uncrewed Aerial Vehicles with Machine Learning Prediction Models. *CEUR Workshop Proceedings*, 3680, 2024. Available at: https://www.scopus.com/inward/record.uri?eid=2-s2.0-85192553885&partnerID=40&md5=24edfd120f416d6aca25d184050016a7.

[17] Nurtas M., Baishemirov Zh., Ydyrys A., Altaibek A. 2-D finite element method using "escript" for acoustic wave propagation. ACM International Conference Proceeding Series, 2020. Available at: https://doi.org/10.1145/3410352.3410774.

[18] Alpar S., Faizulin R., Tokmukhamedova F., Daineko Y. Applications of Symmetry-Enhanced Physics- Informed Neural Networks in High-Pressure Gas Flow Simulations in Pipelines. Symmetry, 16, 5, 2024. Available at: https://doi.org/10.3390/sym16050538.

[19] Nurtas M., Tokmukhamedova F., Ydyrys A., Zhantaev Zh., Nurakynov S., Iskakov B., Altaibek A., Matkerim B. Application of Finite Element Method for Solving Seismoacoustic Modeling Problems in Poroelastic Composite Media. Engineered Science, 26, 2023. Available at: https://doi.org/10.30919/es1030.